

Taylor series representation of the dynamical maps of harmonic RF structures from field data

15-11-2011

R.B. Appleby

The University of Manchester/Cockcroft Institute, UK

In collaboration with

Dan Abell,

Tech-X, USA

Many thanks to Philippe Goudket, Peter McIntosh (EMMA RF cavity)
Graeme Burt, Ben Hall (Crab)

The crab cavity is a beam dynamics device with a complex and non-linear impact on the beam, with the higher order dynamics potentially playing a role at the LHC.

In many studies to date of crab cavity dynamics in the LHC, and also in the standard code PTC, the crab cavity is modelled by the simplified Hamiltonian

$$H_{\text{crab}} = \frac{qV}{P_s} \cdot \sin\left(\frac{\omega z}{c} + \phi\right) x$$

The resulting horizontal canonical momenta kick and the dependent longitudinal kick are given by (using Hamilton's equation)

$$\begin{aligned}\Delta p_x &= -\frac{\partial H_{\text{crab}}}{\partial x} = -\frac{qV}{P_s} \cdot \sin\left(\frac{\omega z}{c} + \phi\right) \\ \Delta p_z &= -\frac{\partial H_{\text{crab}}}{\partial z} = -\frac{qV}{P_s} \cdot \cos\left(\frac{\omega z}{c} + \phi\right) \frac{\omega}{c} \cdot x\end{aligned}$$

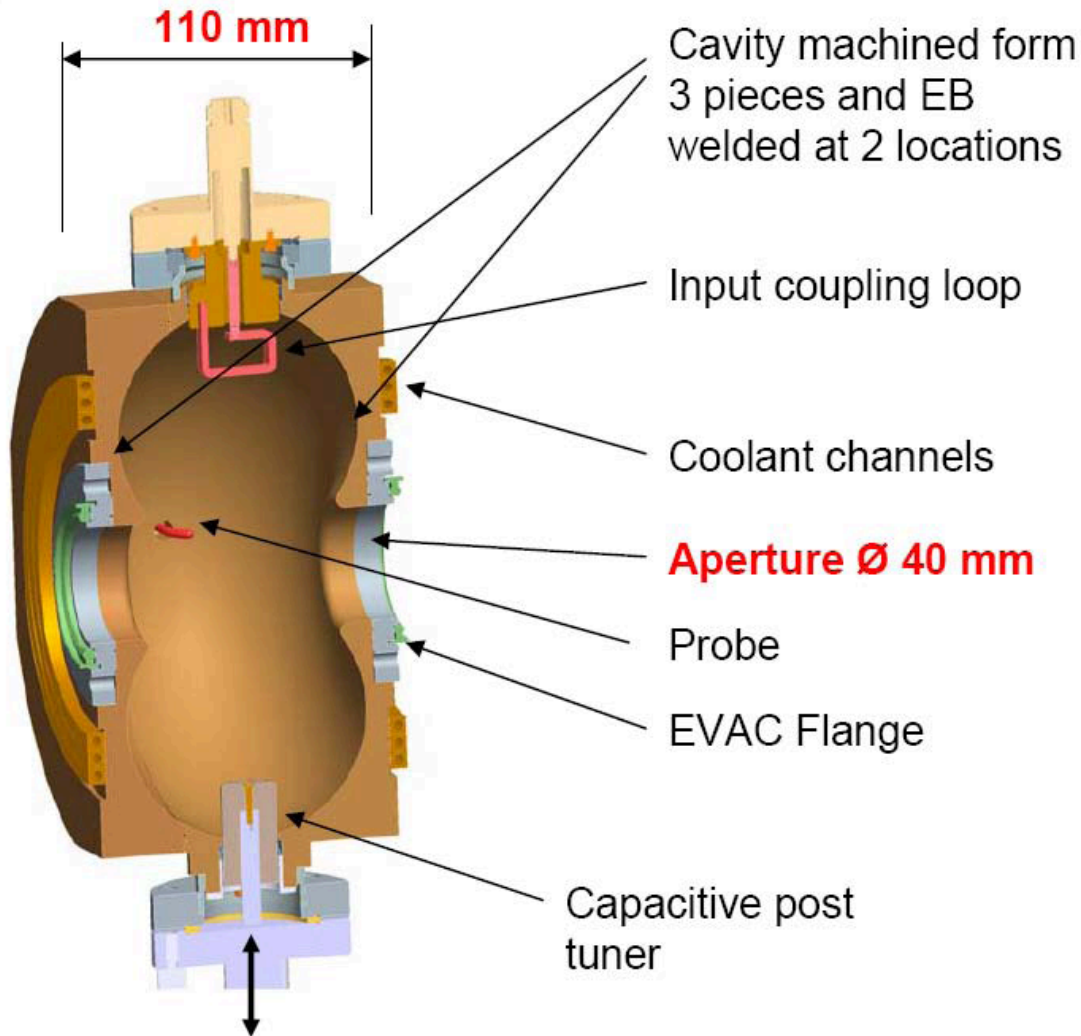
Question for the assembled – what is the complete Hamiltonian of a real crab cavity?

It is possible to take advantage of recent work in the surface fitting of electromagnetic fields and a dynamical map based approach to beam dynamics to model the non-linear behavior of time dependent harmonic structures. (This is complementary to a multipole approach)

Recently, we've studied the dynamical maps of the RF cavity of the EMMA FFAG, with a complete extraction of the cavity's non-linear behaviour from the field map.

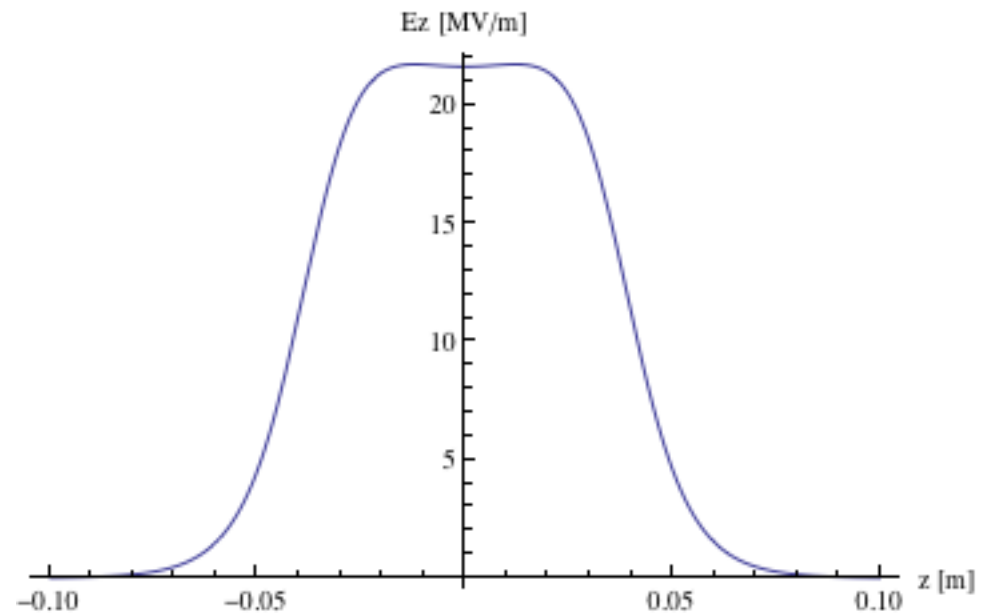
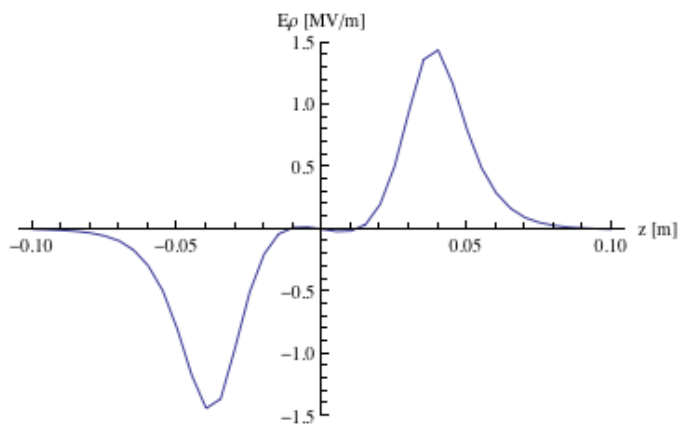
Here, I will present the results for the EMMA RF accelerating cavity and the initial progress for the 4 rod crab cavity.

The EMMA RF cavity



L_{total}	0.2 m
L_{ACC}	0.1 m (central)
$\int E \cdot dx$	1.8 MV
f	1.3 GHz
eV_{eff}	1.08 MeV

The EMMA FFAG at Daresbury (UK) is a non-scaling electron FFAG, with 19 RF cavities. The electric field integral is 1.8 MV from the model, but the cavity is operated at a voltage of 180 keV.



Field fitting

We want the vector potential. We can write (Abell, Phys. Rev. ST Accel. Beams 9, 052001 (2006)) a general solution to the cavity fields, valid inside a region with no sources, in terms of four functions

$$\tilde{e}_m(k) \quad \tilde{f}_m(k) \quad \tilde{\beta}_m(k) \quad \tilde{\alpha}_m(k)$$

We obtain these four functions, valid inside a cylinder inscribed inside the cavity of radius R , using the field components on the surface of this cylinder. Consistency with Maxwell's equations then give the complete solution inside the cylinder. This is surface fitting.

The EMMA RF cavity has a strong azimuthal symmetry, so the equations significantly simplify (which is useful!). Now we only need $e_0(k)$ given in terms of $E_z(r=R)$

$$\tilde{e}_0(k) = \frac{1}{R_0(k, R)} \int_{-\infty}^{\infty} \frac{dz}{\sqrt{2\pi}} e^{-ikz} E_{zc0}(R, z) \quad E_z(\vec{r}) = \int_{-\infty}^{\infty} \frac{dk}{\sqrt{2\pi}} e^{ikz} \tilde{e}_0(k) R_0(r, \rho)$$

The relationship to the analytic vector potential is given through the generalised gradients, which are Fourier transforms of the $e_0(k)$ functions, and are functions of z

$$C_{zc0j}(z) = \int_{-\infty}^{\infty} \frac{dk}{\sqrt{2\pi}} e^{ikz} s_l(k)^j \kappa_l^{2j} \tilde{e}_0(k)$$

The vector potential in the cylinder is then given as a power series in the canonical variables x and y (e.g. for A_z and similarly for A_x and A_y)

$$A_z(x, y, z) = -i \frac{1}{\omega_l} \sum_{j=0}^{\infty} \frac{(x^2 + y^2)^j}{2^{2j} (j!)^2} C_{zc0j}(z)$$

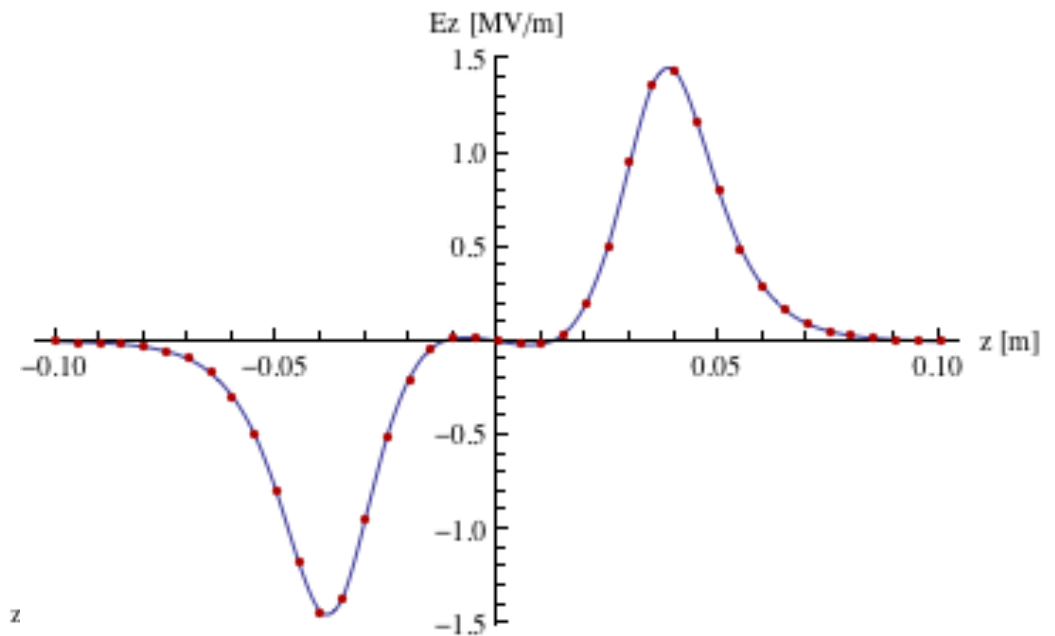
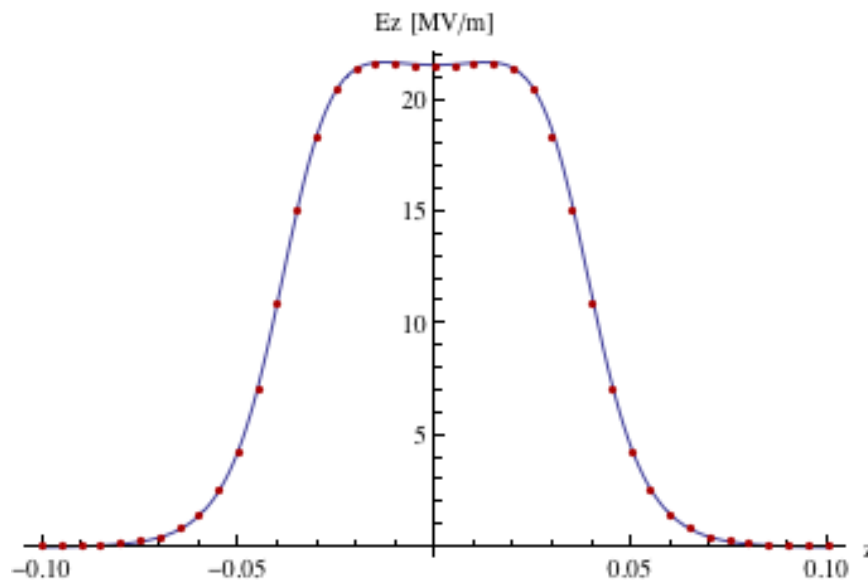
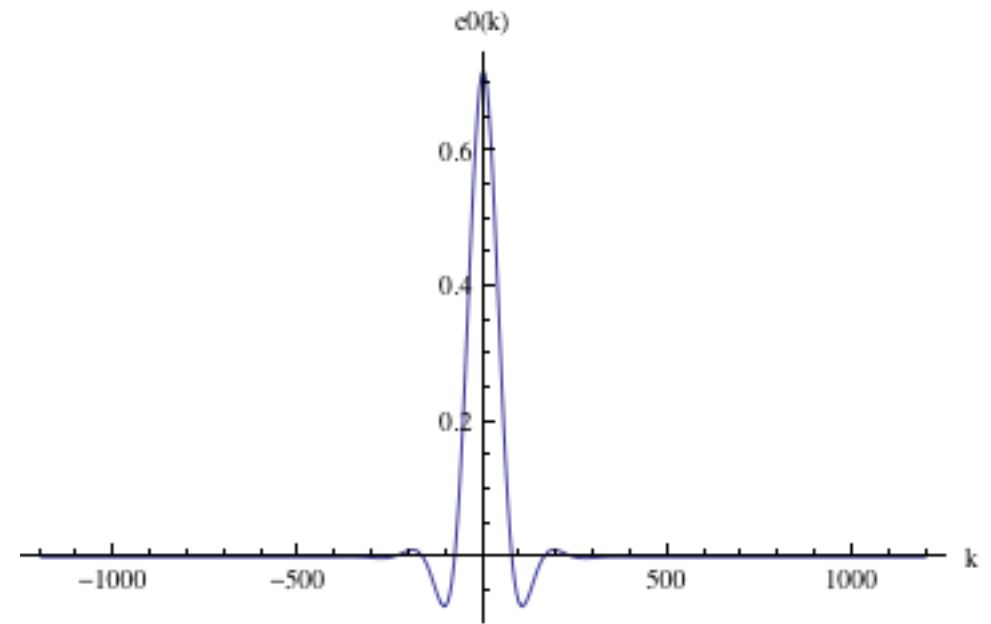
The EMMA cavity $e_0(k)$

The complete calculation for EMMA has been performed (assuming azimuthal symmetry in the cavity).

The field was fitted at $R=17.7$ mm inside a cylinder inscribed in the cavity (avoiding the aperture)

The fitted field at $r=3.5$ mm shows a very good agreement with the known field map at this inner radius.

(blue = data, red = fitted field)



The analytic vector potential for the cavity, which we write as

$$(a_z, a_y, a_s)$$

Can be used to find the Hamiltonian flow, and hence the dynamical maps, of the canonical variables (written in standard form and in extended phase space (Forest *et al*, Phys. Rev. E 68, 046502 (2003))

$$(x, p_x) \quad (y, p_y) \quad (z, \delta) \quad (s, p_s)$$

The Hamiltonian in terms of these canonical variables and these fields takes the form

$$H = -\sqrt{\left(\frac{1}{\beta_0} + \delta\right)^2 - (p_x - a_x)^2 - (p_y - a_y)^2} - \frac{1}{\beta_0^2 \gamma_0^2} - a_s + \frac{\delta}{\beta_0} + p_s$$

The dynamical maps are computed in Taylor form, so writing the 'output' variables after the EMMA cavity as a Taylor series in terms of the 'input' variables. e.g. a sextupole map

$$\begin{aligned} x(s) &= x_0 + sp_{x0} - \frac{1}{4}k_2s^2x_0^2 - \frac{1}{6}s^3x_0p_{x0} - \frac{1}{24}k_2s^4p_{x0}^2 + O(3) \\ p_x(s) &= p_{x0} - \frac{1}{2}k_2sx_0^2 - \frac{1}{2}k_2s^2x_0p_{x0} - \frac{1}{6}k_2s^3p_{x0}^2 + O(3) \end{aligned}$$

The maps are extracted using differential algebra techniques, with the Hamiltonian solved (in the paraxial form) using a split Hamiltonian form and techniques for a s dependent vector potential developed by Forest, Robin and Wu (Phys. Rev. E 68, 046502 (2003))

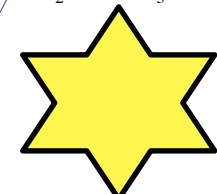
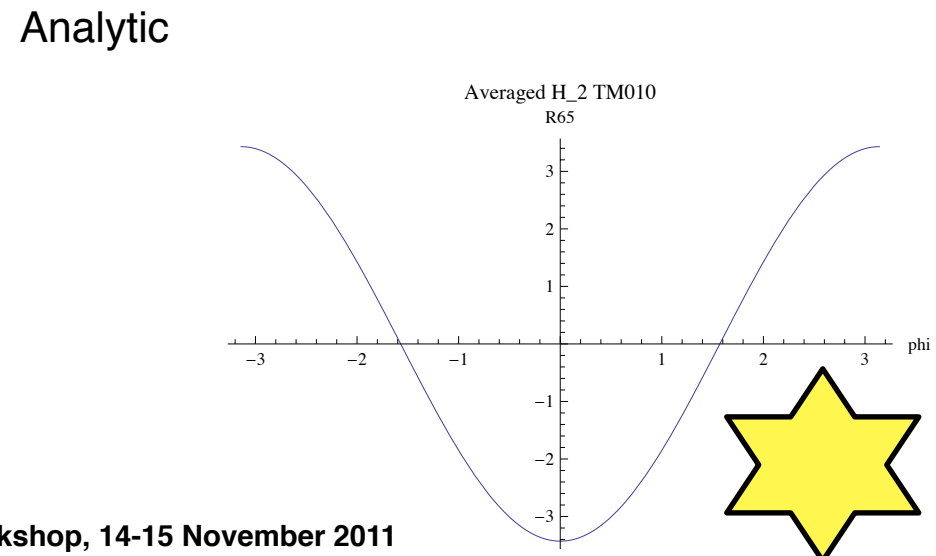
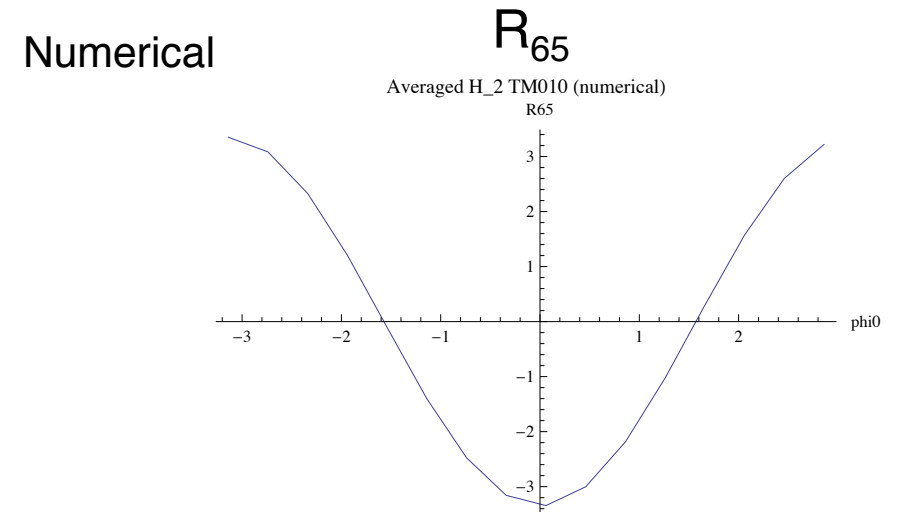
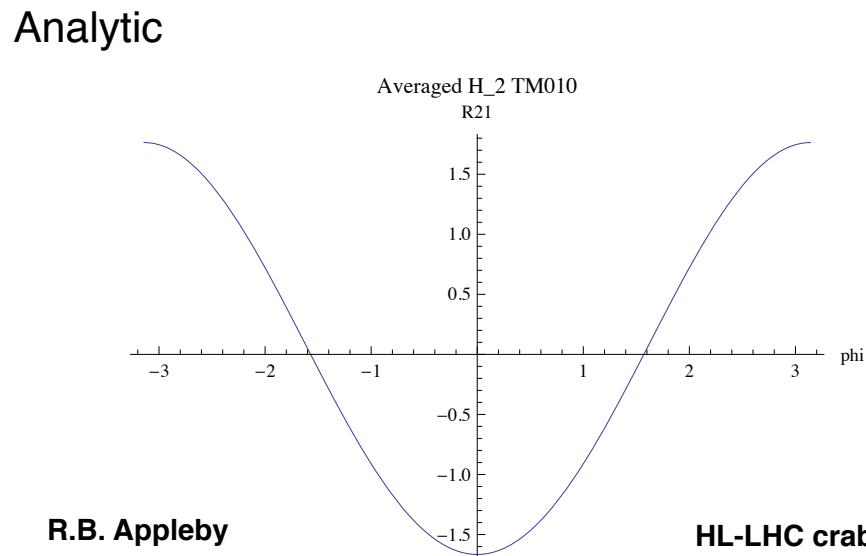
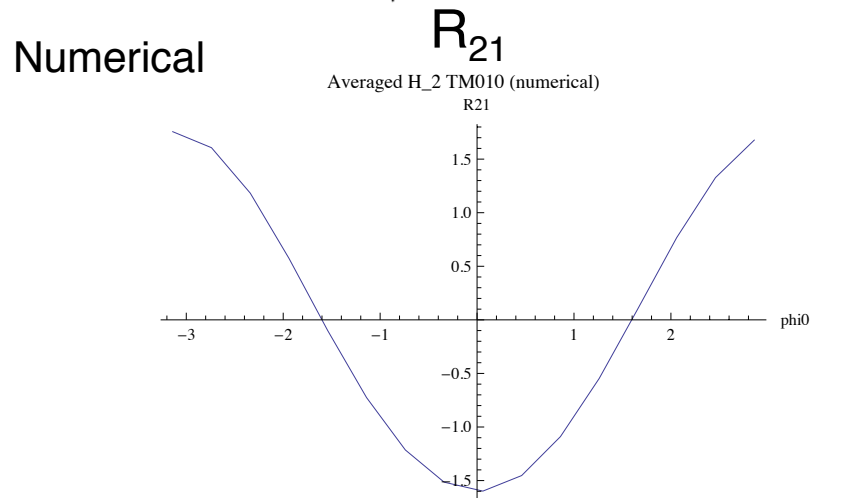
Verification of the integrator

The symplectic integrator can be verified by using the same integrator (formulated in the DA) for a field case with an analytic solution. Pill-box with no beam holes has fields

$$E_\rho = 0 \quad E_\phi = 0 \quad E_s = e_s J_0(k\rho) \sin(\omega t + \phi_0)$$

And can be derived from the Hamilton with a pure longitudinal vector potential

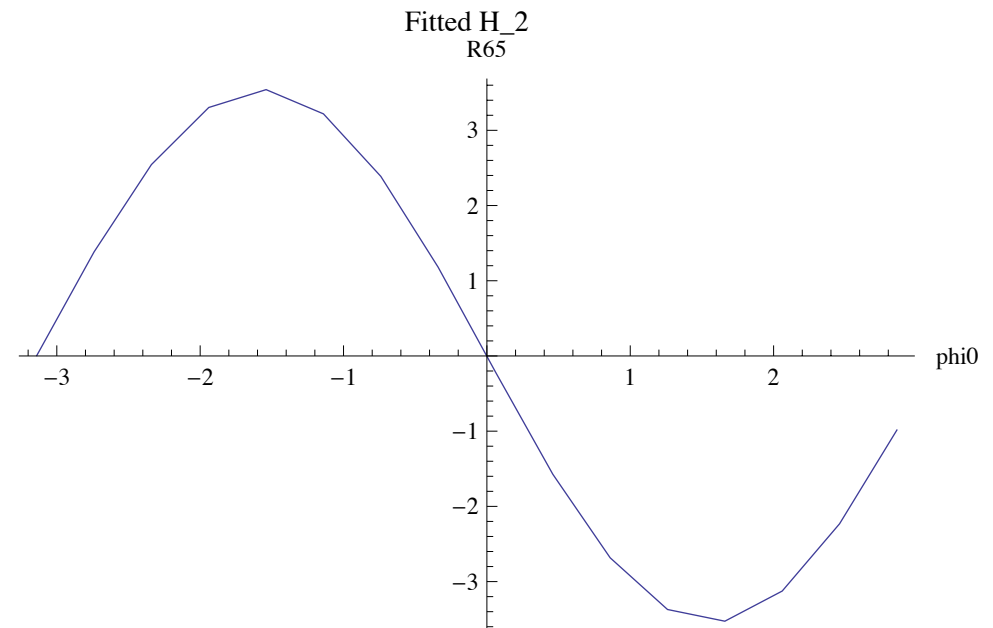
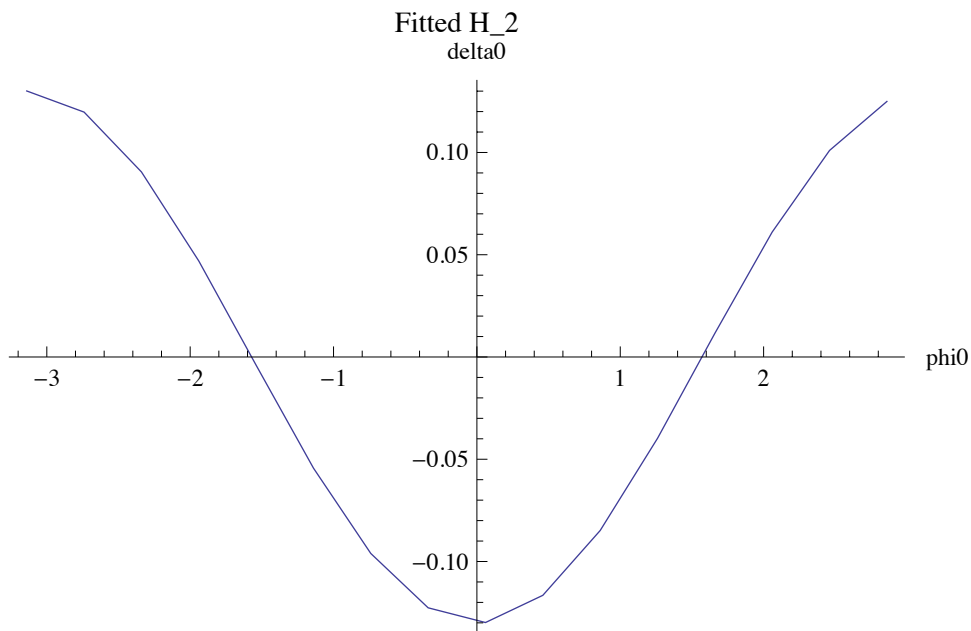
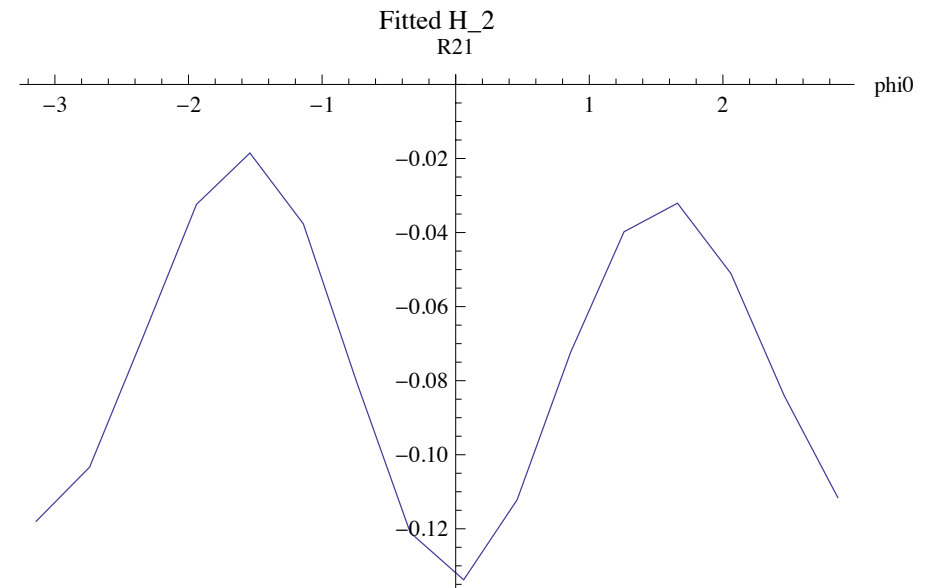
$$H = \frac{\delta}{\beta_0} - \sqrt{\left(\frac{1}{\beta_0} + \delta\right)^2 - p_x^2 - p_y^2} - \frac{1}{\beta_0^2 \gamma_0^2} - \frac{q}{P_0} \frac{e_s}{\omega} J_0(k\rho) \cos\left(\frac{k}{\beta_0} s - kz + \phi_0\right)$$



EMMA cavity linear maps

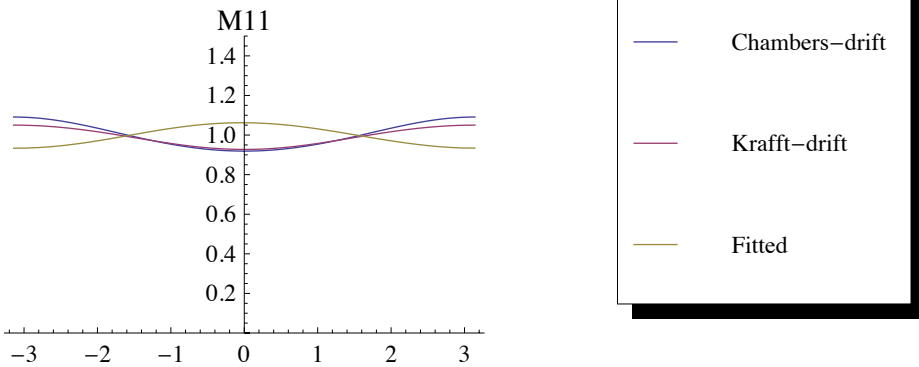
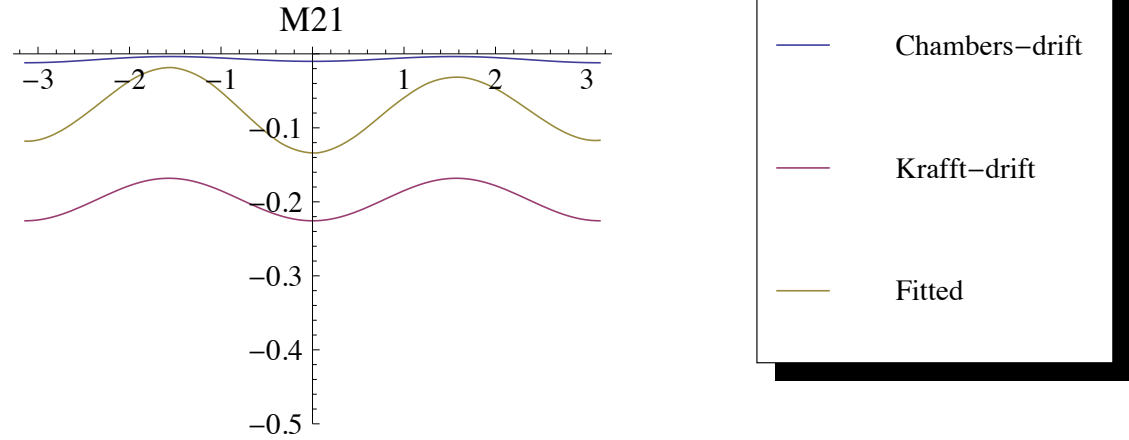
Now we can calculate the dynamical map of the EMMA cavity in Taylor series form using the analytic fitted vector potential. The parts of this map linear in the dynamical variables correspond to the standard linear transfer matrices.

The constant term corresponds to the change in relative momentum of the particle through the cavity, or acceleration

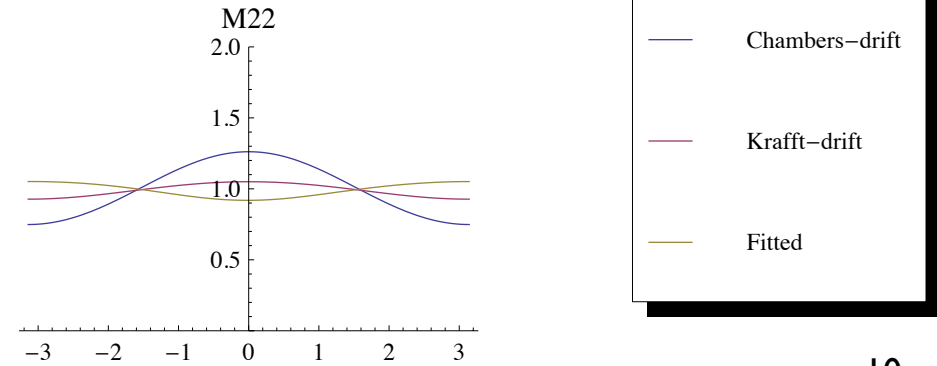
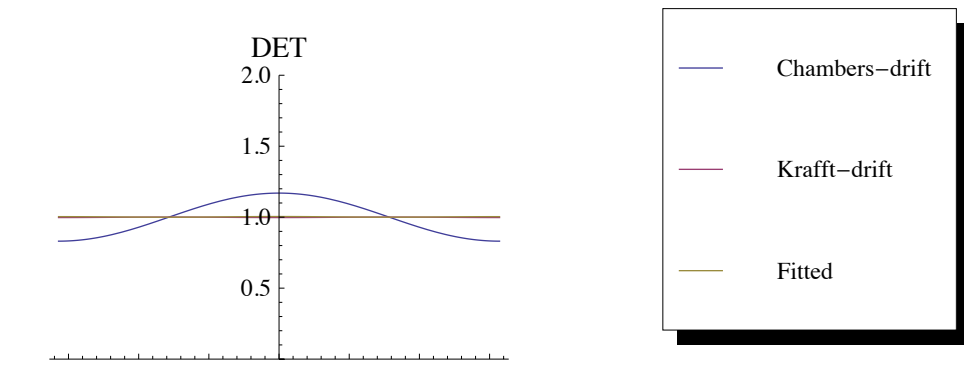


Cavity linear maps : comparison to Krafft and Chambers models

There are many RF cavity transverse focusing models, many of which can be derived from the model of Rosenzweig and Sarafini. Two common models for a resonant cavity with $\beta=1$ are the Chambers and the Krafft models, which predict the transverse focusing linear transfer map.



The transverse focusing behaviour of the EMMA cavity show the same functional form between the two models and the fitted map, with an uncertainty in the normalisation. The fitted map lies between the Chambers and the Krafft model predictions. The uncertainty in M_{21} between the Chambers and Krafft models was studied for the CEBAF cavity and attributed to ‘approximations made for higher energy beams’.



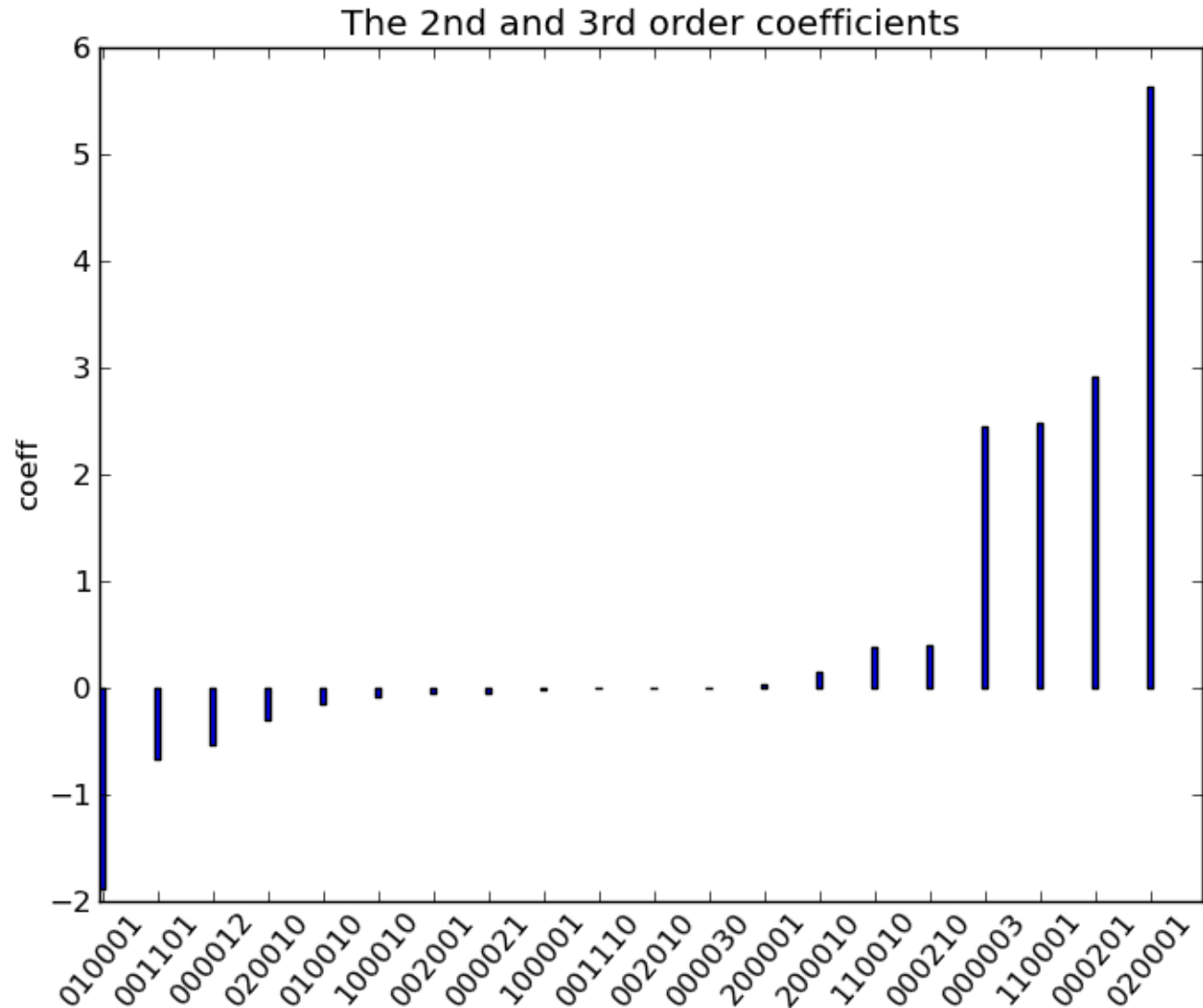
The higher order terms in the Taylor series representation of the map we extract from the calculation corresponds to the higher order, non-linear behavior of the cavity.

Here we show the largest 2nd and 3rd order coefficients for the EMMA cavity at the maximally accelerating phase. Note we have both transverse, longitudinal and coupled coefficients.

Notation is the power of the dynamical variable, in order

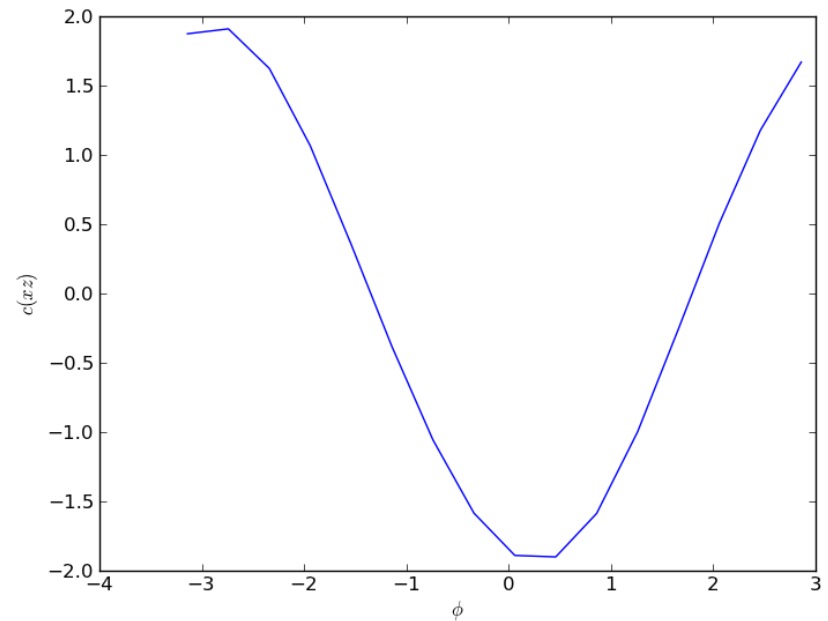
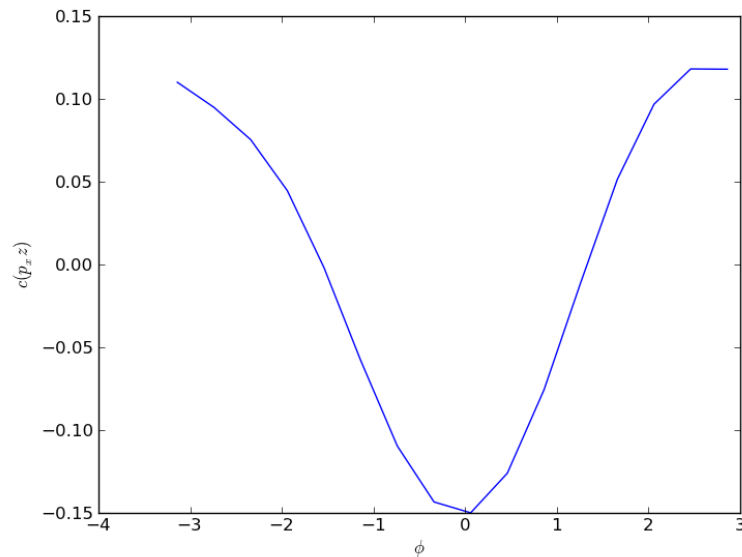
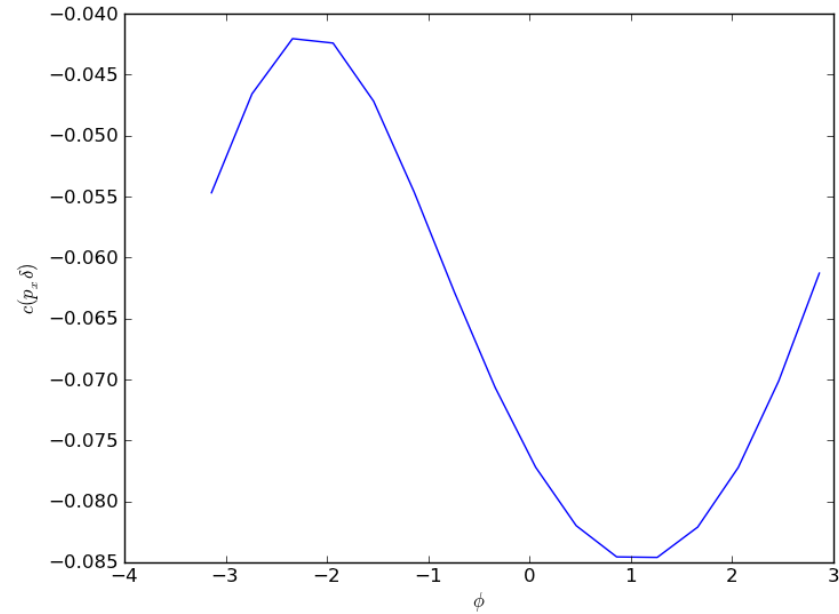
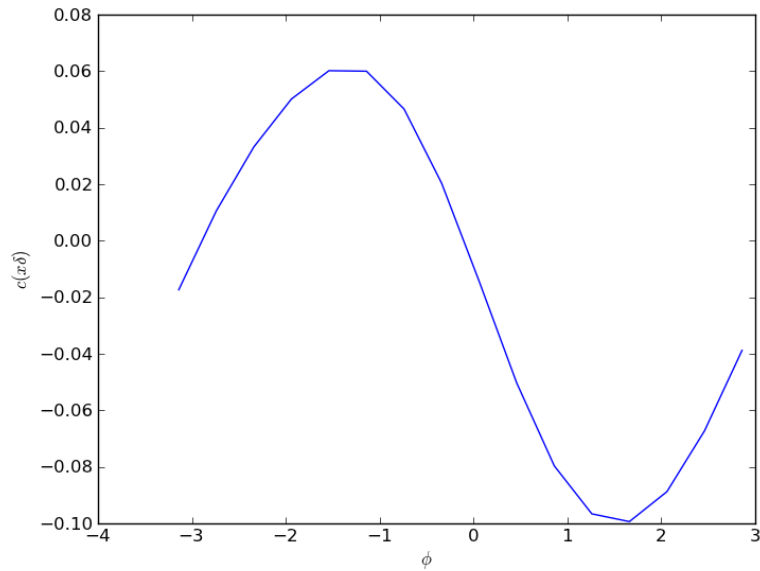
(Delta z p_y y p_x x)

e.g. 010001 means the coefficient of z¹ x¹ in the map and corresponds to transverse-longitudinal 2nd order coupling



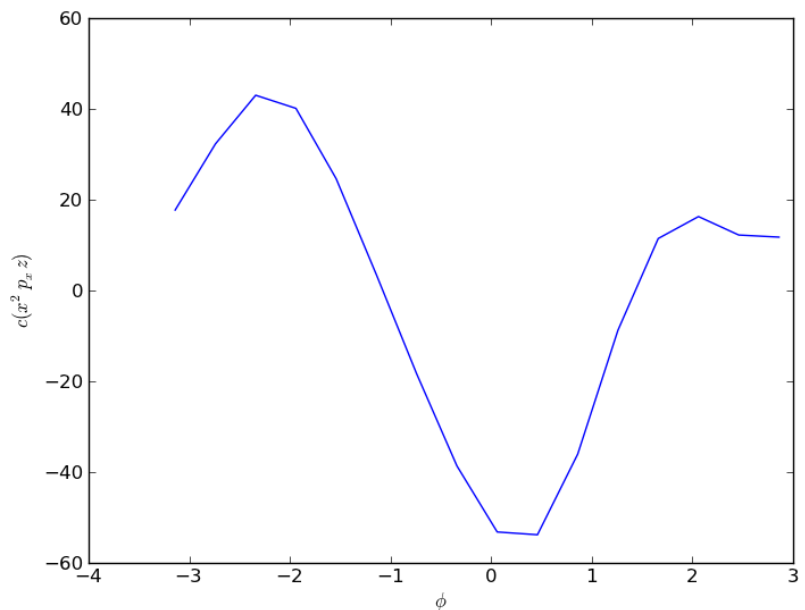
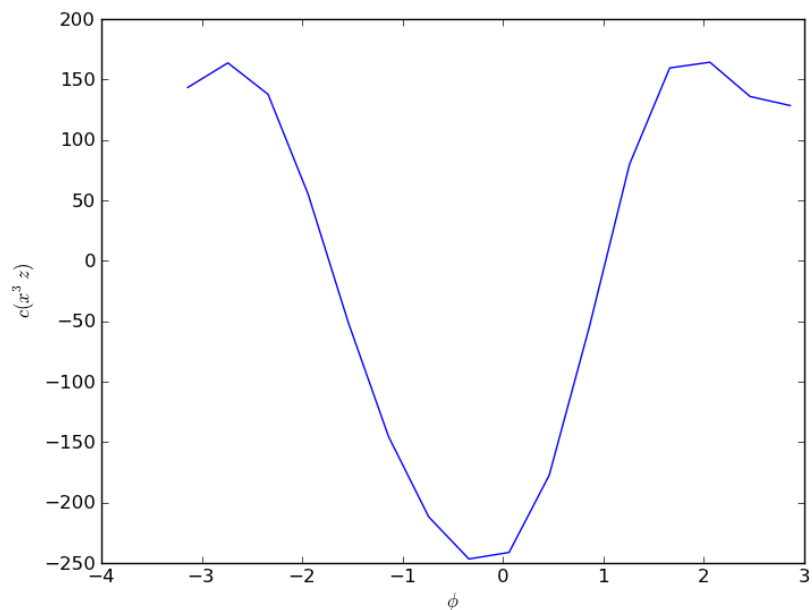
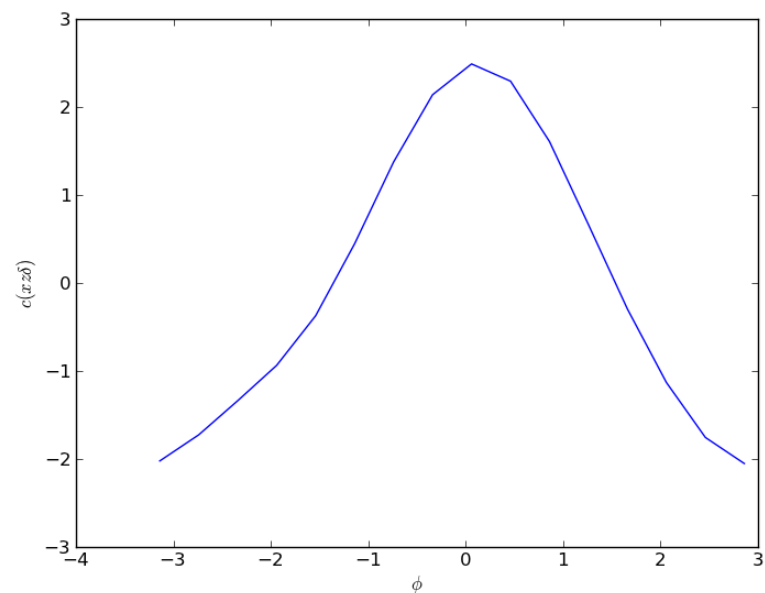
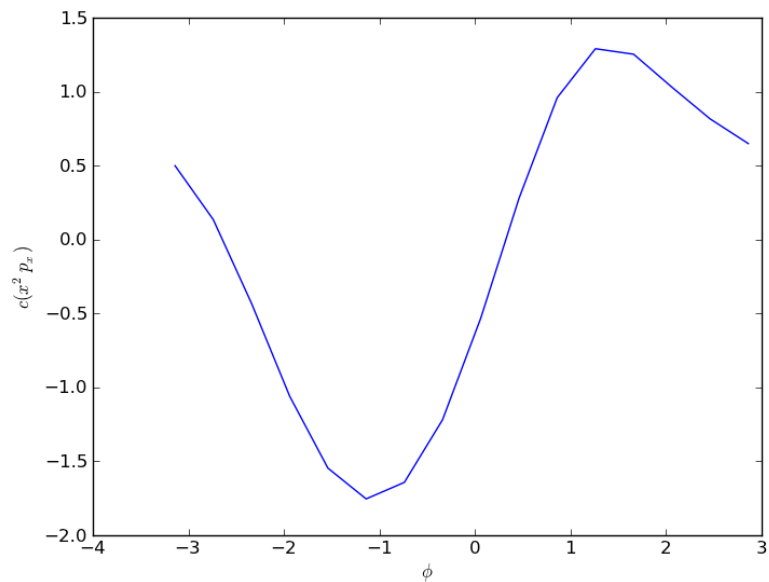
2nd order map coefficients as a function of cavity phase

We can also pick out the dominant 2nd order coefficients in the map and study their behavior as a function of phase. Again we treat transverse and longitudinal effects equally.



3rd and 4th order map coefficients as a function of cavity phase

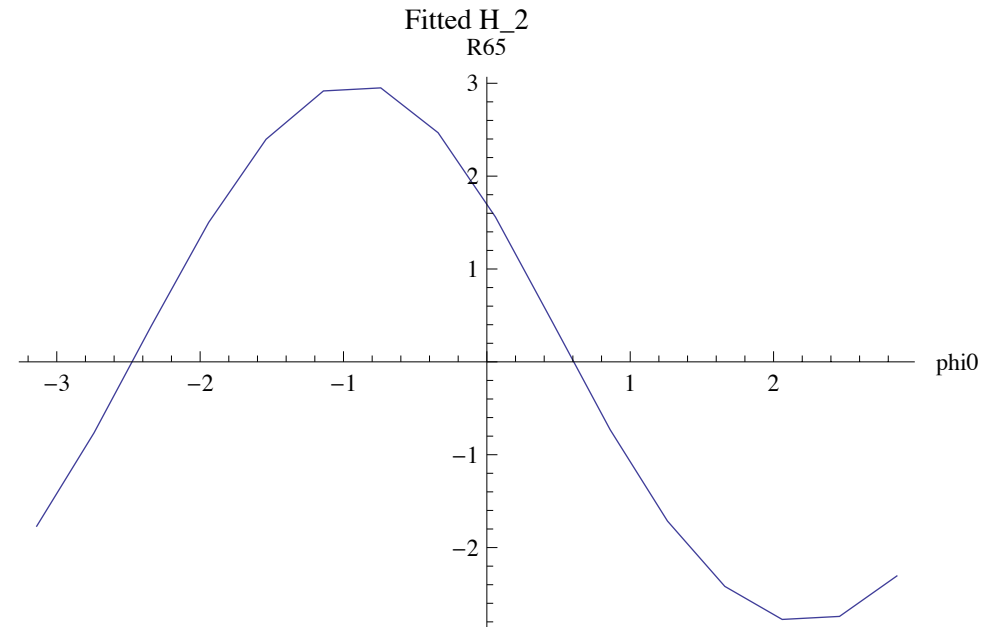
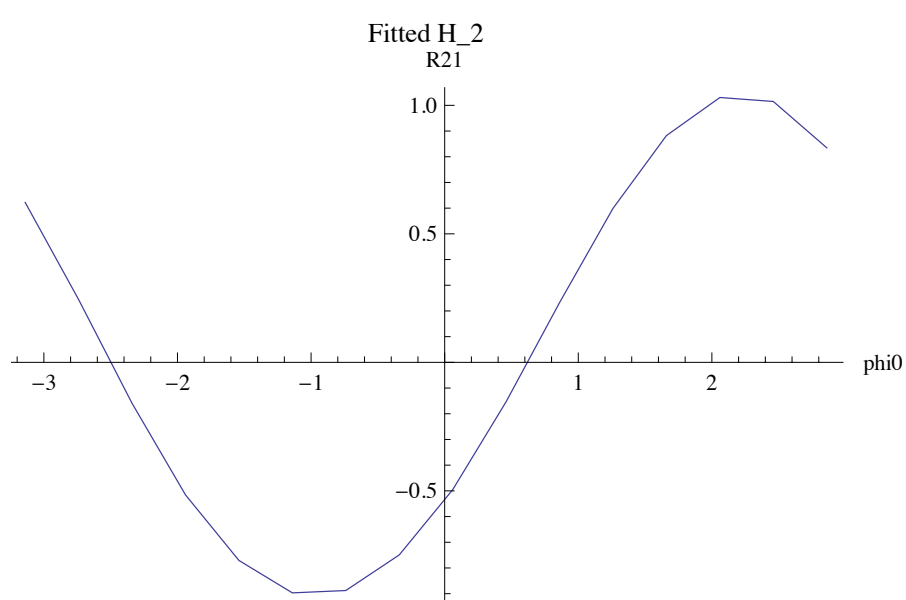
And, for fun, we can also pick out the dominant 3rd order coefficients in the map and study their behavior as a function of phase.



The linear maps for beta < 1

The calculation is also valid at non-relativistic particle velocities, so we can calculate the linear and non-linear maps for the cavity for a particle with $v \ll c$.

For example, the transverse and longitudinal matrix elements R_{21} and R_{65} for a particle with a velocity of 0.65

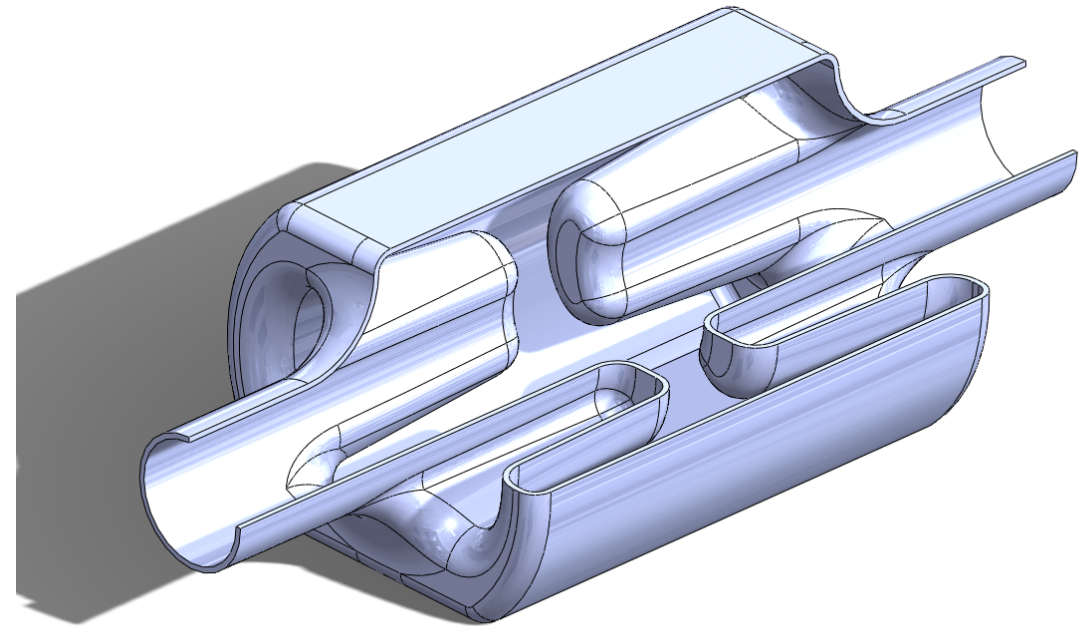


4 bar crab cavity

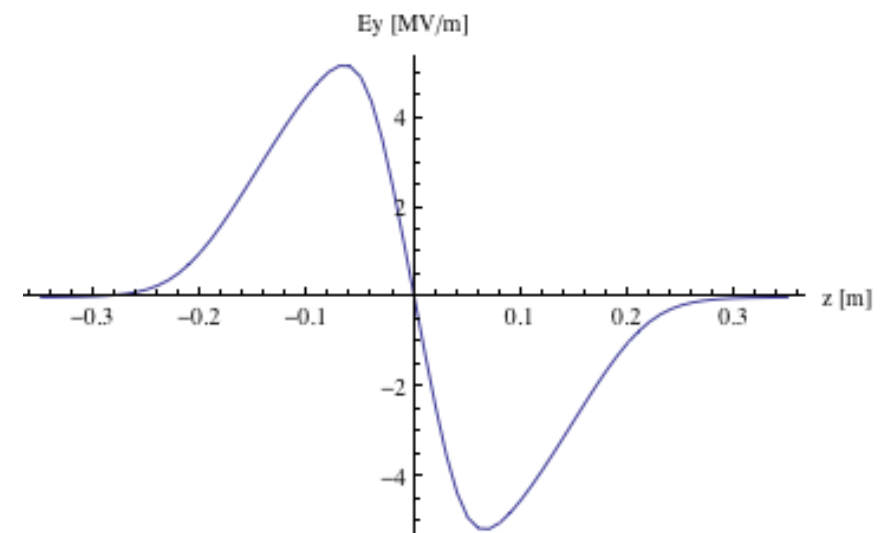
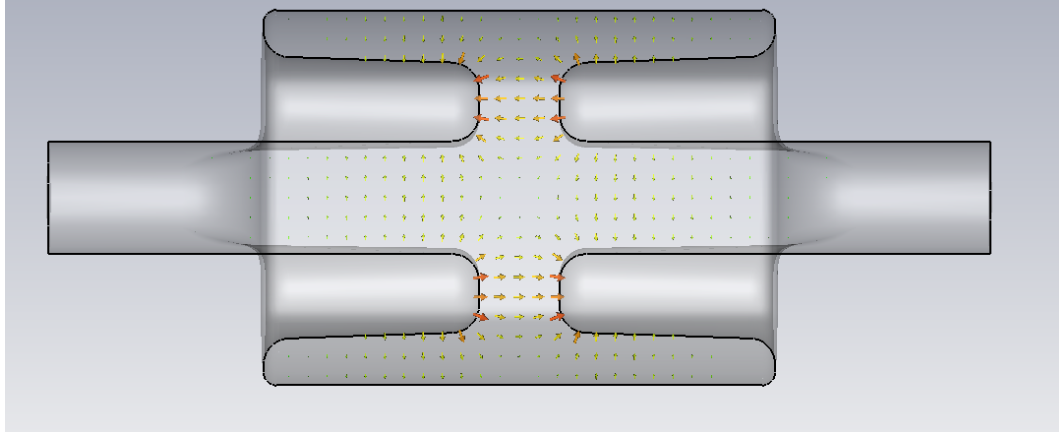
The four rod cavity is a crabbing structure using a TEM mode to crab the LHC beam. It operates at 400 MHz. The crabbing is done with electric and magnetic fields.

This is a cavity designed by the Cockcroft Institute (see talks by G Burt and B Hall) so is a nice place to start looking at the linear and non-linear beam dynamics of the a crab cavity through dynamical maps.

The result will be a full map for the cavity as a function of particle phase.



The electric field of the crabbing mode



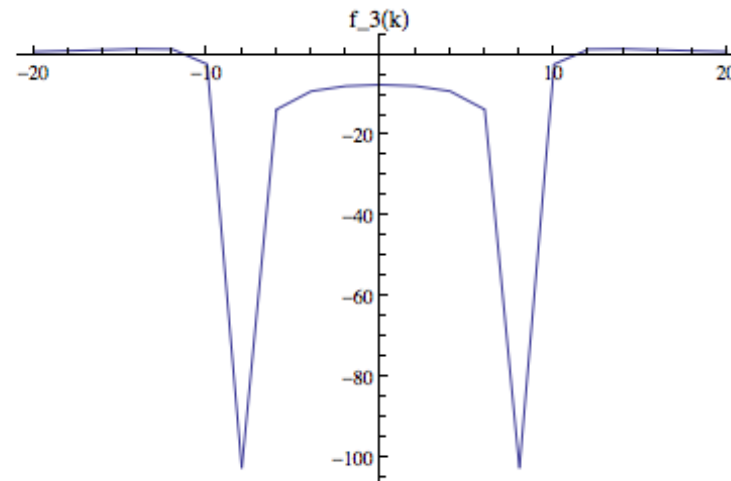
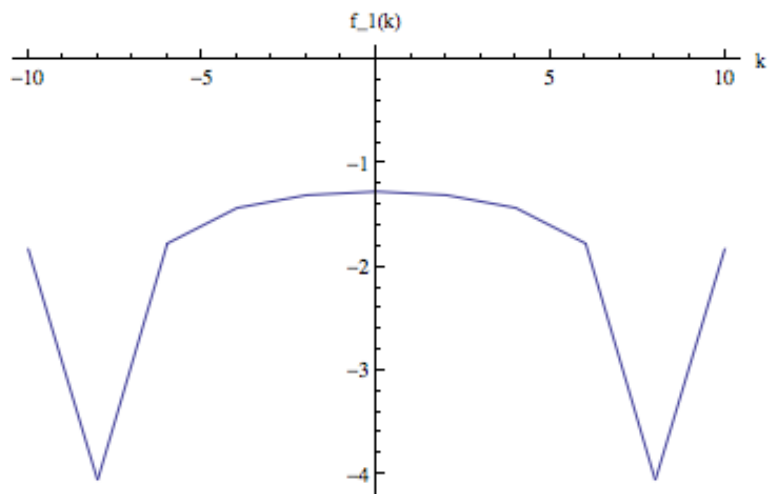
The 4-rod crab cavity

The cavity is not azimuthally symmetric, so we need all the fitting functions to fully describe the solution of the Helmholtz equation in the cavity body.

We use the longitudinal electric field on the surface of a cylinder of radius 3 cm, avoiding the four cavity rods in the structure.

The field fitted on this surface then provides the field inside this cylinder.

So far (last two weeks) we've shown that $e_m(k)=0$ for all m for this cavity design, and computed $f_k(m)$ for $m > 0$.



In the remaining part of the year we should complete the coefficients, completely model the field and begin to extract the dynamical maps as a function of phase in 2012.

- The crab cavity, whatever the design, has a non-linear effect on the beam and a complete modelling of higher order behaviour may be crucial for the beam dynamics studies of the crab in the LHC and may help with cavity design.
 - For example, DA studies in the LHC
 - Interaction with collimation system
 - Non-linear z-dependent dispersion (already studied linearly, arises from z dependent transverse kick)

- We've used field fitting techniques developed for magneto-static transverse beam dynamics to calculate a fitted vector potential for a RF accelerating cavity and used differential algebra techniques to extract the resulting dynamical map as a function of phase in Taylor series representation.

- The technique gives the non-linear impact of the cavity on the beam, and is valid for all particle velocities.

- We've currently calculating the maps for the 4 rod crab cavity.
 - This is work on progress as we can't exploit any azimuthal symmetry
 - These map can be used for dynamical studies, assessment of higher order behaviour and even as an input to cavity design.
 - These maps can be easily added to codes like PTC.

There are many RF cavity transverse focusing models, many of which can be derived from the model of Rosenzweig and Sarafini.

Two common models for a resonant cavity with $\beta=1$ are the Chambers and the Krafft models, which predict the transverse focusing linear transfer map.

$$m_{11} = 1 - \frac{\cos(\phi) \int_{-\infty}^{+\infty} E_z(z) \cos(\omega z/c) dz}{2\gamma_i m c^2} \quad m_{12} = L/\gamma_i$$

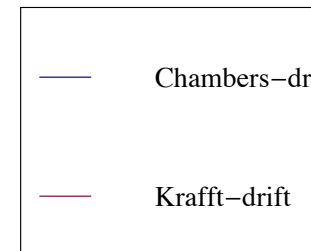
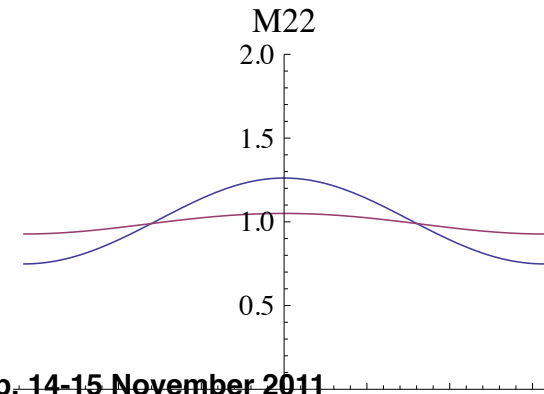
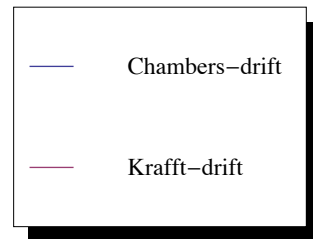
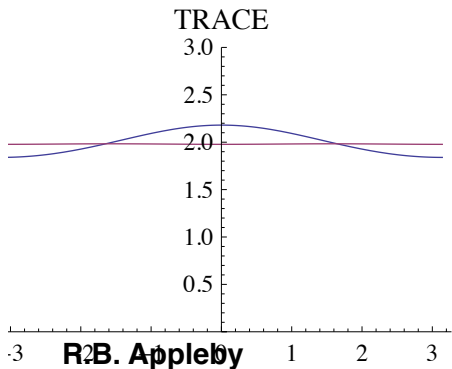
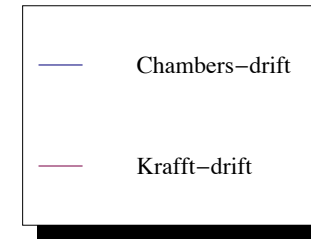
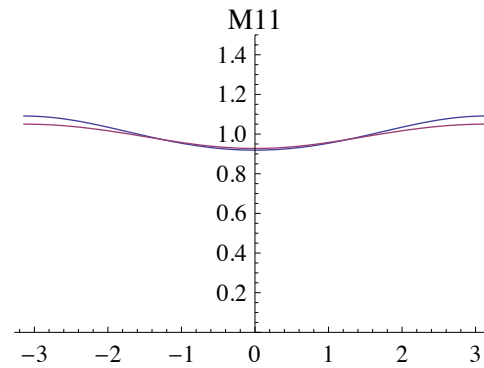
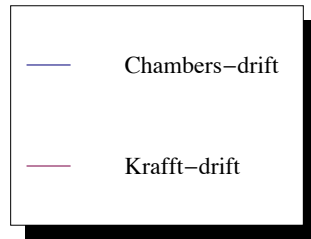
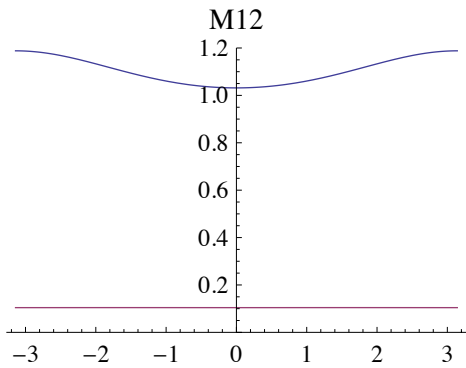
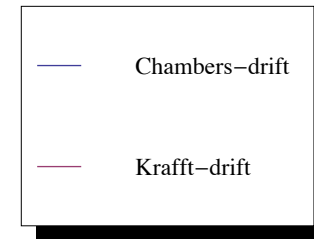
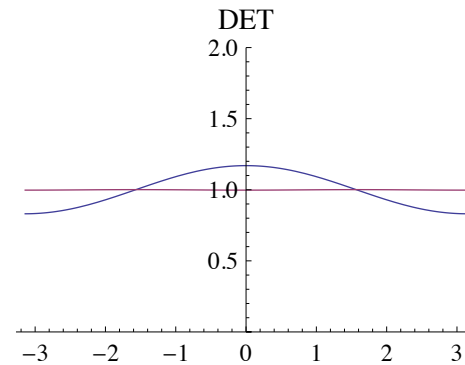
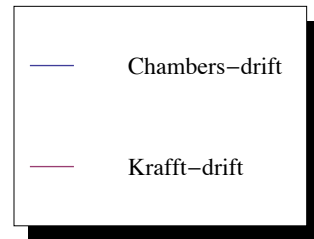
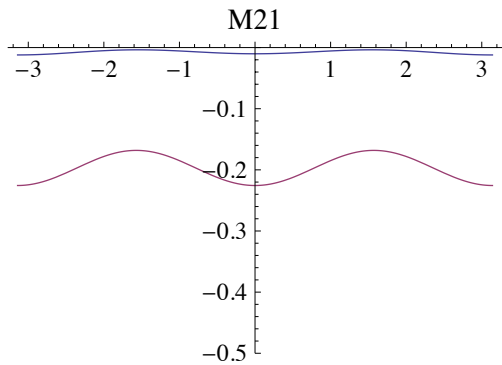
$$m_{21} = -\frac{1}{4\gamma_i} \left(\cos^2(\phi) \int_{-\infty}^{+\infty} E_z^2(z) \cos^2(\omega z/c) dz + \sin^2(\phi) \int_{-\infty}^{+\infty} E_z^2(z) \sin^2(\omega z/c) dz \right)$$

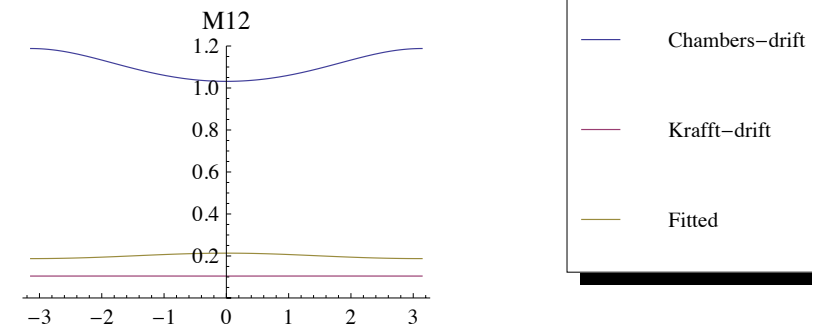
$$m_{22} = 1 + \frac{\cos(\phi) \int_{-\infty}^{+\infty} E_z(z) \cos(\omega z/c) dz}{2\gamma_i m c^2}$$

$$M_t = \begin{pmatrix} \cos(\alpha) - \sqrt{2} \cos(\phi) \sin(\alpha) & \sqrt{8} \frac{\gamma_i}{\gamma_f} \cos(\phi) \sin(\alpha) \\ -\frac{\gamma_f'}{\gamma_f} \left(\frac{\cos(\phi)}{\sqrt{2}} + \frac{1}{\sqrt{8} \cos(\phi)} \right) \sin(\alpha) & \frac{\gamma_i}{\gamma_f} [\cos(\alpha) + \sqrt{2} \cos(\phi) \sin(\alpha)] \end{pmatrix}$$

$$\alpha = \left(\frac{\sqrt{1/8}}{\cos(\phi)} \right) \log \left(\frac{\gamma_f}{\gamma_i} \right).$$

The Chambers and Krafft models : comparison





$$e^{-h:(p_x - a_x)^2} = \hat{A}_x e^{-h:p_x^2} \hat{A}_x^{-1} \hat{A}_x = e^{-\int a_x(x', y, z) dx'}$$

To extract the dynamical map for the cavity we fit an analytic vector potential to the electromagnetic fields obtained from a field map. These obey the wave equation (written for the electric field)

$$\nabla^2 \vec{E} - \frac{1}{c^2} \frac{\partial^2 \vec{E}}{\partial t^2} = 0$$

Assuming a harmonic time dependence for the electric field,

$$\vec{E}(\vec{r}, t) = \sum_l \vec{E}^{(l)}(\vec{r}) e^{-i(\omega_l t + \phi)}$$

The spatial part of the electric field obeys the Helmholtz equation mode by mode

$$\nabla^2 \vec{E}^{(l)}(\vec{r}) + k_l^2 \vec{E}^{(l)}(\vec{r}) = 0 \quad k_l = \omega_l / c$$

It can then be shown (Abell, Phys. Rev. ST Accel. Beams 9, 052001 (2006)) that we can write a general solution to this equation, valid inside a region with no sources, in terms of four functions

$$\tilde{e}_m(k) \quad \tilde{f}_m(k) \quad \tilde{\beta}_m(k) \quad \tilde{\alpha}_m(k)$$

We obtain these four functions, valid inside a cylinder inscribed inside the cavity of radius R , using the electric field components on the surface of this cylinder. Consistency with Maxwell's equations then give the complete solution inside the cylinder. For example,

$$\tilde{e}_m(k) = \frac{1}{R_m(k, R)} \int_{-\infty}^{\infty} \frac{dz}{\sqrt{2\pi}} e^{-ikz} E_{zcm}(R, z) = \frac{\tilde{E}_{zcm}(R, k)}{R_m(k, R)}$$

The EMMA RF cavity has a strong azimuthal symmetry, so these equations significantly simplify (which is useful!). Now we only need $e_0(k)$ given in terms of $E_z(r=R)$

$$\tilde{e}_0(k) = \frac{1}{R_0(k, R)} \int_{-\infty}^{\infty} \frac{dz}{\sqrt{2\pi}} e^{-ikz} E_{zc0}(R, z)$$

And we can write the electric field anywhere in the cylinder as,

$$E_z(\vec{r}) = \int_{-\infty}^{\infty} \frac{dk}{\sqrt{2\pi}} e^{ikz} \tilde{e}_0(k) R_0(r, \rho)$$

The relationship to the analytic vector potential is given through the generalised gradients, which are Fourier transforms of the $e_0(k)$ functions, and are functions of z

$$C_{zc0j}(z) = \int_{-\infty}^{\infty} \frac{dk}{\sqrt{2\pi}} e^{ikz} s_l(k)^j \kappa_l^{2j} \tilde{e}_0(k)$$

The vector potential in the cylinder is then given as a power series in the canonical variables x and y (e.g. for A_z and similarly for A_x and A_y)

$$A_z(x, y, z) = -i \frac{1}{\omega_l} \sum_{j=0}^{\infty} \frac{(x^2 + y^2)^j}{2^{2j} (j!)^2} C_{zc0j}(z)$$

Where we define

$$s_l(k) = \text{sgn}(k^2 - k_l^2) \quad \kappa_l^2 = |k^2 - k_l^2|$$

Verification of the integrator

The symplectic integrator can be verified by using the same integrator (formulated in the DA) for EMMA and also for a known case with an analytic solution. Pill-box with no beam holes has fields

$$E_\rho = 0 \quad E_\phi = 0 \quad E_s = e_s J_0(k\rho) \sin(\omega t + \phi_0)$$

And can be derived from the Hamilton with a pure longitudinal vector potential

$$H = \frac{\delta}{\beta_0} - \sqrt{\left(\frac{1}{\beta_0} + \delta\right)^2 - p_x^2 - p_y^2} - \frac{1}{\beta_0^2 \gamma_0^2} - \frac{q}{P_0} \frac{e_s}{\omega} J_0(k\rho) \cos\left(\frac{k}{\beta_0} s - kz + \phi_0\right)$$

This Hamiltonian can be integrated using the same DA method as the EMMA cavity to calculate the linear part of the dynamical map. This can be compared to the analytic solution for this system

$$R = \begin{pmatrix} \cos(\psi_\perp) & \frac{L}{\psi_\perp} \sin(\psi_\perp) & 0 & 0 & 0 & 0 \\ -\frac{\psi_\perp}{L} \sin(\psi_\perp) & \cos(\psi_\perp) & 0 & 0 & 0 & 0 \\ 0 & 0 & \cos(\psi_\perp) & \frac{L}{\psi_\perp} \sin(\psi_\perp) & 0 & 0 \\ 0 & 0 & -\frac{\psi_\perp}{L} \sin(\psi_\perp) & \cos(\psi_\perp) & 0 & 0 \\ 0 & 0 & 0 & 0 & \cos(\psi_\parallel) & \frac{1}{\beta_0^2 \gamma_0^2} \frac{L}{\psi_\parallel} \sin(\psi_\parallel) \\ 0 & 0 & 0 & 0 & -\beta_0^2 \gamma_0^2 \frac{\psi_\parallel}{L} \sin(\psi_\parallel) & \cos(\psi_\parallel) \end{pmatrix}$$

Where we have defined

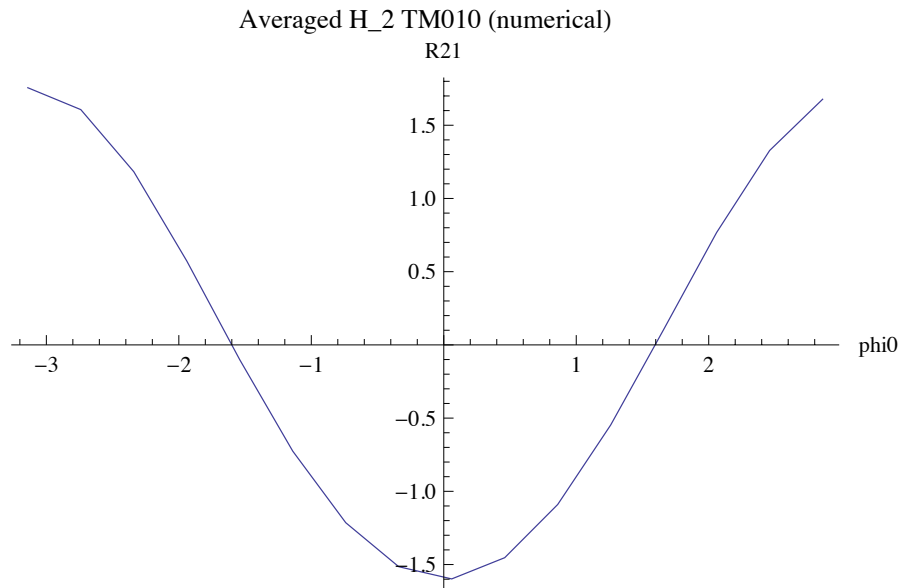
$$\psi_\perp = \sqrt{\frac{\pi \alpha \cos(\phi_0)}{2}} \quad \psi_\parallel = \frac{\sqrt{\pi \alpha \cos(\phi_0)}}{\gamma_0 \beta_0} \quad c_z = \frac{2}{\pi} L \sin^2\left(\frac{\psi_\perp}{2}\right) \tan \phi_0$$

$$c_\delta = \alpha \frac{\sin \psi_\perp}{\psi_\perp} \sin \phi_0$$

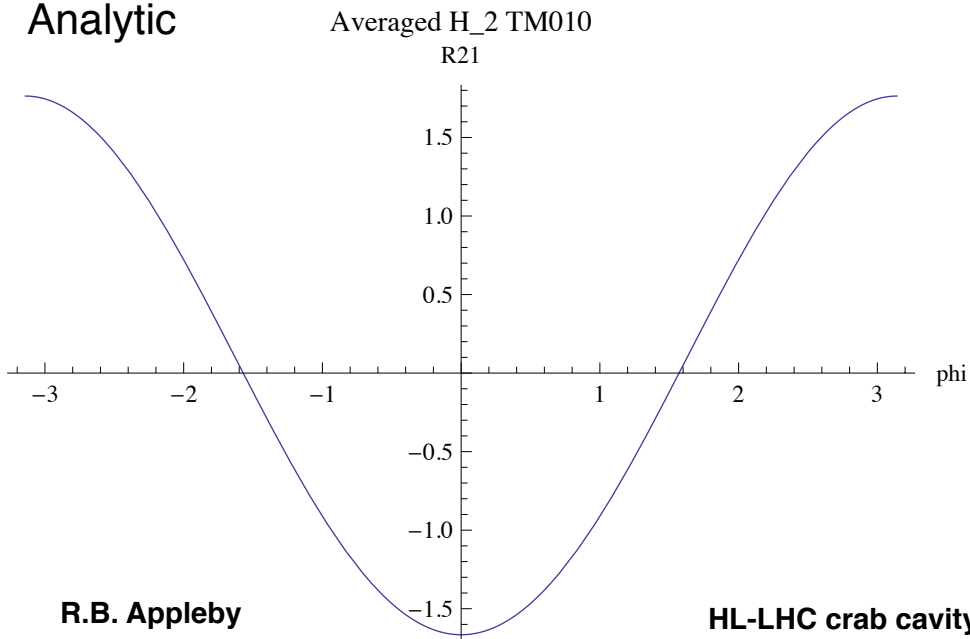
Verification of the integrator

R_{21}

Numerical



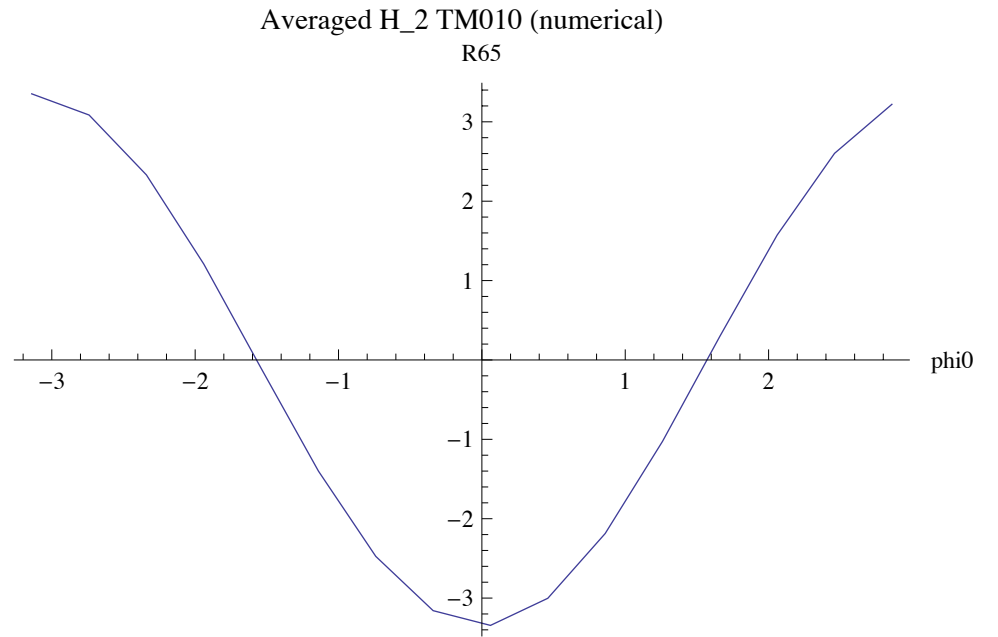
Analytic



R.B. Appleby

R_{65}

Numerical



Analytic

